Dictyostelium ACAP-A is an ArfGAP involved in cytokinesis, cell migration and actin cytoskeleton dynamics

Marco Dias[1], Cédric Blanc[1], Nelcy Thazar-Poulot[2,3,4,5,6], Sabrina Ben Larbi[3,4,7], Pierre Cosson[1] and François Letourneur[3,4,7,*]

[1]Département de Physiologie Cellulaire et Métabolisme, Centre Médical Universitaire, 1 rue Michel Servet, 1211 Geneva 4, Switzerland
[2]CNRS, UMR5667, UMS3444, 15 parvis René Descartes BP 7000, Lyon, 69342, France
[3]Université de Lyon, Lyon, 69361, France
[4]Université Lyon 1, Villeurbanne, 69622, France
[5]Ecole Normale Supérieure de Lyon, Lyon, 69342, France
[6]Institut National de la Recherche Agronomique, Lyon, 69364, France
[7]CNRS, UMR5534, Centre de Génétique et de Physiologie Moléculaire et Cellulaire, 16 rue Raphaël Dubois, Villeurbanne, 69622, France
*Author for correspondence (francois.letourneur@univ-lyon1.fr)

Accepted 19 November 2012
Journal of Cell Science 126, 756–766

doi: 10.1242/jcs.113951

Summary

ACAPs and ASAPs are Arf-GTPase-activating proteins with BAR, PH, GAP and ankyrin repeat domains and are known to regulate vesicular traffic and actin cytoskeleton dynamics in mammalian cells. The amoeba *Dictyostelium* has only two proteins with this domain organization, instead of the six in human, enabling a more precise functional analysis. Genetic invalidation of *acapA* resulted in multinucleated cells with cytokinesis defects. Mutant *acapA*$^{-}$ cells were hardly motile and their multicellular development was significantly delayed. In addition, formation of filopodial protrusions was deficient in these cells. Conversely, re-expression of ACAP-A–GFP resulted in numerous and long filopodia-like protrusions. Mutagenesis studies showed that the ACAP-A actin remodeling function was dependent on its ability to activate its substrate, the small GTPase ArfA. Likewise, the expression of a constitutively active ArfA•GTP mutant in wild-type cells led to a significant reduction in filopodia length. Together, our data support a role for ACAP-A in the control of the actin cytoskeleton organization and dynamics through an ArfA-dependent mechanism.

Key words: ArfGAP, Cytokinesis, Migration, Actin cytoskeleton

Introduction

The ADP-ribosylation factor (Arf) proteins are GTP-binding proteins that control vesicular transport and remodeling of the actin cytoskeleton (D'Souza-Schorey and Chavrier, 2006; Gillingham and Munro, 2007; Donaldson and Jackson, 2011). These proteins cycle between active GTP-bound and inactive GDP-bound forms with distinct functions. The tight control of this cycle relies on two key families of proteins. Arf-Guanine nucleotide exchange factors (Arf-GEFs) catalyze the exchange of GDP, whereas Arf-GTPase activating proteins (Arf-GAPs) induce hydrolysis of GTP bound to Arf proteins. Besides their catalytic functions, both GEFs and GAPs can serve as scaffold for numerous effector proteins and can thus regulate cellular physiology in an Arf-independent manner (Inoue and Randazzo, 2007; Randazzo et al., 2007).

In humans, 31 predicted ArfGAPs have been classified into ten subfamilies (Kahn et al., 2008). In addition to a GAP domain, four subfamilies (ASAP, ACAP, AGAP and ARAP), comprising 20 proteins have a pleckstrin homology (PH) and ankyrin (ANK) repeat domains. ASAP and ACAP subfamilies each include three members and exhibit at their N-terminus a BAR domain (Bin, Amphiphysin and Rvs). ASAPs contain an additional SH3 domain at their C-termini. Both ASAPs and ACAPs mainly function as regulator of the actin cytoskeleton dynamics (Inoue and Randazzo, 2007; Randazzo et al., 2007). ASAPs associate with three distinct cytoskeletal structures, focal adhesions, circular dorsal rufles and invadopodia/podosomes but their precise role in the formation and the dynamics of these structures is still largely unknown. ACAPs regulate Arf6-dependent actin remodeling (Inoue and Randazzo, 2007). For instance both ACAP1 and ACAP2 associate with Arf6-induced endocytic tubules and plasma membrane protrusions (Jackson et al., 2000). In addition, ACAP1 function as part of an Arf6-regulated clathrin vesicular coat involved in endocytic recycling of integrin beta 1 that is critical for cell migration (Li et al., 2005; Li et al., 2007). More recently, ACAP2 was shown to associate with Rab35 (Kanno et al., 2010) and ACAP2 recruitment on Arf6-positive endosomes through Rab35 regulates Arf6-dependent neurite outgrowth of PC12 cells (Kobayashi and Fukuda, 2012).

In the social amoeba *Dictyostelium discoideum*, there are only 12 genes with a predicted Arf-GAP domain (Chen et al., 2010). ASAP, AGAP and ARAP proteins are missing but two proteins (ACAP-A and -B) are highly homologous to human ACAPs (Gillingham and Munro, 2007; Chen et al., 2010). These two proteins are GAPs for ArfA, the only member of the Arf protein

family identified in the *Dictyostelium* genome based on protein sequence comparison studies (Weeks et al., 2005; Chen et al., 2010). ACAP-A and ACAP-B have been proposed to share redundant functions since the deletion of both genes is necessary to induce relatively minor defects in spore biogenesis and in actin dynamics during multicellular development (Chen et al., 2010). These observations were quite surprising considering the critical role of mammalian ASAPs and ACAPs in actin cytoskeleton remodeling and membrane trafficking.

Filopodia are long (<10 μm) and thin (0.1–0.2 μm) finger-like membrane protrusions involved in various cellular processes such as cell adhesion, chemotaxis, and development (Wood and Martin, 2002). Filopodia contain tight parallel bundles of actin filaments with their barded ends pointing towards filopodial tips. In *Dictyostelium*, filopodia consist of a discontinuous actin filaments network aligned in parallel or obliquely to the filopodium shaft and the tip region comprises about ten short actin filaments arranged to form a 'terminal cone' (Medalia et al., 2007). Filopodia formation has been shown to be driven by the assembly of actin filaments. Thus actin nucleation appears as a key event in the initiation of filopodia, although the actual nucleation mechanism is still controversial (Faix and Rottner, 2006; Gupton and Gertler, 2007; Mattila and Lappalainen, 2008; Faix et al., 2009; Ahmed et al., 2010; Mellor, 2010; Yang and Svitkina, 2011). Two major mechanisms of initiation have been proposed based on two distinct actin filament nucleators, the Arp2/3 complex and formins. In the 'convergent elongation' model, filopodia form from the elongation of pre-existing lamellipodial actin filaments induced by the activation of nucleation-promoting factors such as WASP/WAVE-family proteins that in turn activate the Arp2/3 complex. Conversely, in the 'tip nucleation' model, formins are proposed to ensure actin nucleation and polymerisation at filopodial tips. Recent studies suggest that both the Arp2/3 complex and formins could collaborate in filopodia initiation (Block et al., 2012; Breitsprecher et al., 2012). In addition, several proteins including IRSp53 (Ahmed et al., 2010) and Myosin X (Kerber and Cheney, 2011) have been shown to contribute to filopodia formation suggesting that multiple mechanisms of filopodia formation might exist in different cell types. In *Dictyostelium*, filopodia form mainly by actin tip nucleation since the Arp2/3 complex is dispensable for their formation (Steffen et al., 2006) and the Diaphanous related formin, dDia2 is required for their extension (Schirenbeck et al., 2005). Although Rac1 interacts with dDia2 (Schirenbeck et al., 2005), the respective and coordinated functions of Rho and Arf GTPases in filopodia formation in *Dictyostelium* cells are mostly unknown.

In this study we explored the function of the *Dictyostelium* ACAP-A protein. *Dictyostelium* is a genetically tractable eukaryotic cell with remarkable membrane remodeling capacities, as seen for instance during cell migration and phagocytosis. The presence of only two proteins exhibiting PH, Arf-GAP and ANK domains makes this organism an attractive cellular model to study the function of Arf-GAP proteins without functional redundancy problems inherent to the presence of numerous Arf-GAPs, as observed in human. Our results indicate that ACAP-A, but not ACAP-B, is specifically involved in cytokinesis, cell motility and actin cytoskeleton remodeling, in an Arf-dependent manner. These new functions of ACAP-A were not reported before, mainly because they were not assayed in previous studies (Chen et al., 2010).

Results

acapA^{-} cells exhibit impaired cytokinesis

To explore the function of ACAP-A, the corresponding gene was disrupted in *Dictyostelium* cells by targeted integration of the blasticidin selection marker. Several independent clones were analyzed and showed identical phenotypes, described hereafter. Disruption was confirmed by genomic PCR and RT-PCR. In addition, immunoblotting of whole cell lysates with an ACAP-A specific anti-peptide confirmed that the ACAP-A protein was not present in *acapA*$^{-}$ cells, whereas stable transfection of GFP-tagged ACAP-A led to overexpression of ACAP–A-GFP compared to the endogenous expression level in wild-type cells (Fig. 1A). As observed in Fig. 1B, *acapA*$^{-}$ cells showed a larger and more heterogenous size than wild-type (WT) cells. To determine if the large size of *acapA*$^{-}$ cells was the consequence

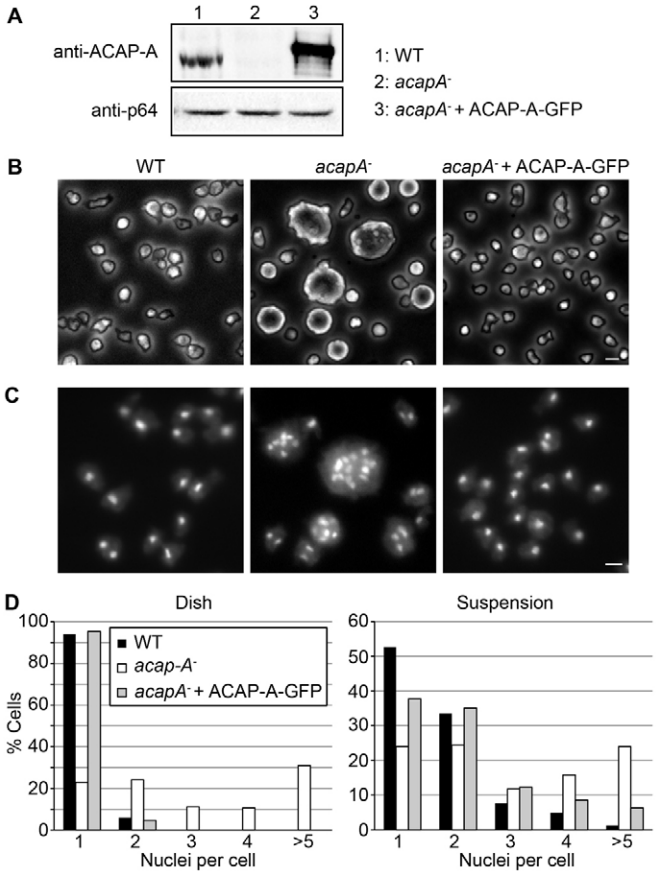

Fig. 1. Morphological characterization and nuclei analysis of *acapA*$^{-}$ cells. (**A**) Whole cell lysates (10^6 cells/lane) were analyzed by electrophoresis (7% polyacrylamide gel) and ACAP-A revealed with an anti-ACAP-A specific rabbit anti-peptide. Identical amounts of protein were loaded in each lane as verified by immunoblotting with an anti-p64 rabbit antibody. ACAP-A was not detected in *acapA*$^{-}$ cells, whereas *acapA*$^{-}$ cells transfected with GFP-tagged ACAP-A overexpressed the tagged protein. Calculated molecular weights for ACAP-A and GFP-tagged ACAP-A were respectively 146 and 173 kDa. (**B**) Wild-type (WT), *acapA*$^{-}$ and mutant cells transfected with GFP-tagged ACAP-A (*acapA*$^{-}$ + ACAP-A-GFP) were observed by phase-contrast microscopy or (**C**) grown overnight on glass coverslips, fixed and stained with DAPI. Scale bar: 10 μm. (**D**) Histograms showing the distribution of nuclei/cell among wild-type (black), *acapA*$^{-}$ (white) and *acapA*$^{-}$ + ACAP-A–GFP (grey) cells grown in plastic Petri-dishes and in suspension for 4 days at 180 r.p.m. as indicated (n=500 cells). Results are from one representative experiment repeated at least twice.

of a failure in cytokinesis, the number of nuclei per cell was analyzed after DNA staining of fixed cells with 4′,-6-diamidino-2-phenylindole (DAPI) (Fig. 1C). Whereas 94% of WT cells growing on a plastic substrate contained a single nucleus, 77% of *acapA*$^{-}$ showed two or more nuclei (Fig. 1D, left panel), indicating a defect in cytokinesis. Similarly, *acapA*$^{-}$ cells grown in suspension for four days also exhibited a cytokinesis defect (51.6% of *acapA*$^{-}$ cells with more than two nuclei versus 13.8% for WT cells) (Fig. 1D, right panel). When *acapA*$^{-}$ cells were stably transfected with GFP-tagged ACAP-A, a normal cell size and number of nuclei were restored (Fig. 1B–D). *acapB*$^{-}$ cells did not show cytokinesis defects (supplementary material Fig. S1A) pointing out that even if ACAP-A and ACAP-B both have ArfGAP activities (Chen et al., 2010), ACAP-A shows distinct and specific functions.

To analyze the cytokinesis defect of *acapA*$^{-}$ cells, time-lapse video microscopy observations were performed on cells grown for 24 hours on glass coverslips. Wild-type cells completed cytokinesis within 180 seconds after cell rounding up (supplementary material Fig. S2A). Constriction of the equatorial cleavage furrow started after 90 seconds followed by the formation of an intercellular bridge (120–150 seconds) and abscission (180 seconds). One representative example of defective cytokinesis observed with *acapA*$^{-}$ cells is shown in supplementary material Fig. S2B. Cell rounding up occurred, but one of the presumptive daughter cells seemed to detach from the substrate and stayed above the other daughter cell for 600 seconds. At the 660 seconds frame, both presumptive daughter cells attached to the substrate and deep furrowing was observed in the equatorial region. This equatorial furrowing lasted for 120 seconds before the furrow regressed and the daughter cells eventually merged into a single cell containing probably at least two nuclei. Aborted abscission of daughter cells was also observed in large multinucleated *acapA*$^{-}$ cells (supplementary material Fig. S2C). These time-lapse observations confirm that cytokinesis is defective in *acapA*$^{-}$ and suggest that ACAP-A might participate in constriction of the equatorial cleavage furrow and/or abscission mechanisms. Although cytokinesis defects were not previously reported in *acapA*$^{-}$/*B*$^{-}$ double null cells (Chen et al., 2010), our results are in agreement with observations made in human cells in which depletion of ACAP1 similarly results in cytokinesis inhibition (Rueckert and Haucke, 2012).

To determine whether ACAP-A localized to the cleavage furrow, we made use of *acapA*$^{-}$ cells expressing ACAP-A–GFP since ACAP-A–GFP fully complemented the cytokinesis defect of *acapA*$^{-}$ cells indicating that the fusion protein was functional. In interphase cells, ACAP-A–GFP was seen in the cytosol and was enriched at the cell cortex (Fig. 2). In mitotic cells detected by anti-tubulin staining, ACAP-A–GFP did not accumulate at the level of the cleavage furrow or the midbody. Instead, ACAP-A–GFP appeared still mainly in the cytosol and slightly enriched in pericentrosomal regions in some cells. Like in mammalian cells, in *Dictyostelium* cytokinesis is dependent on the remodeling of the actin cytoskeleton, and many mutants with altered actin cytoskeleton exhibit cytokinesis defects (Gebbie et al., 2004). Our observations suggest that, like ACAP proteins in mammalian cells, ACAP-A may be specifically required to regulate the organization of the actin cytoskeleton.

In *Dictyostelium*, ArfA is the only ArfGTPase (Weeks et al., 2005; Chen et al., 2010). Protein sequence alignment (program

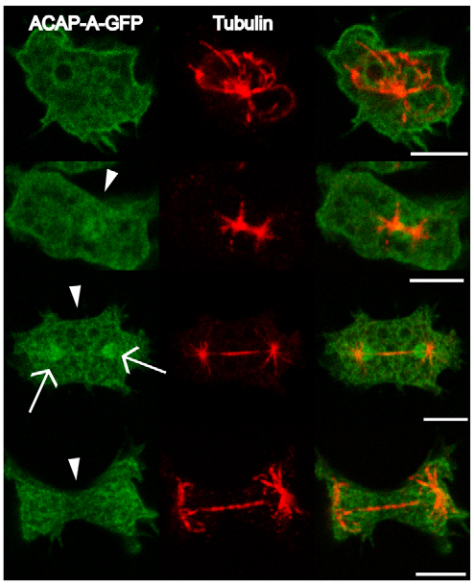

Fig. 2. ACAP-A–GFP localization in mitotic cells. *acapA*$^{-}$ + ACAP-A–GFP cells were labeled with anti-tubulin antibody to detect mitotic cells and analyzed by confocal microscopy. In interphase cells (upper row), ACAP-A–GFP localized in the cytosol and at the cell surface. In mitotic cells, ACAP-A–GFP did not accumulate on cleavage furrows (indicated by arrowheads) but was slightly enriched in pericentrosomal regions (indicated by arrows) in some cells. Scale bars: 5 μm.

EMBOSS Needle, EMBL-EBI) with representative members of the three classes of mammalian Arfs revealed that ArfA shared 83% identity and 88.5% similarity with human Arf1 (class I), 80.8% identity and 87.4% similarity with human Arf4 (class II), and 64.3% identity and 78.6% similarity with human Arf6 (class III). This high homology with class I/II human Arfs suggests that ArfA might participate in the same cellular functions as these human proteins. However, due to its significant similarity with Arf6, ArfA might also play additional roles in actin cytoskeleton dynamics and endocytic processes, as described for Arf6 (D'Souza-Schorey and Chavrier, 2006; Gillingham and Munro, 2007; Donaldson and Jackson, 2011). In mammalian cells, Arf6 is also required for cytokinesis and constitutively active Arf6 localizes to the plasma membrane at the site of cleavage furrow ingression and midbody formation prior to the separation of the daughter cells (Schweitzer and D'Souza-Schorey, 2002). Since ArfA is a substrate for ACAP-A (Chen et al., 2010), we next determined ArfA distribution during mitosis. To avoid massive overexpression of ArfA, we transfected cells with plasmids that allow inducible expression, upon doxycycline addition (Veltman et al., 2009), of ArfA-Q71L or ArfA-T31N mutants fused to GFP at their C-terminus. These mutations mimic respectively constitutively activated (Arf•GTP) and dominant negative (Arf•GDP) forms of human Arf1 that is the closest homolog of ArfA (see above). After 48 hours of induction, ArfA mutants were equally expressed in stably transfected WT cells (Fig. 3A) and 17.9% of cells expressing ArfA-Q71L–GFP showed two nuclei or more against 3.1% of ArfA-T31N–GFP expressing cells (Fig. 3B). This cytokinesis defect induced by expression of constitutively active ArfA is similar to that described in mammalian cells upon overexpression of a GTPase-defective

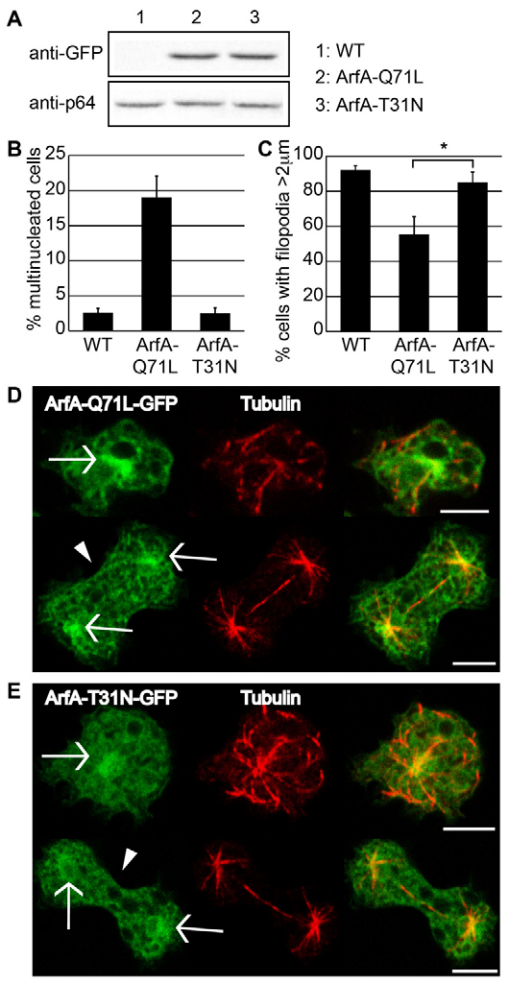

Fig. 3. ArfA localization during cytokinesis and defects induced by ArfA•GTP overexpression. (**A**) ArfA-GFP mutants were equally expressed in cells. Whole cell lysates (5×10^5 cells/lane) were analyzed by electrophoresis (10% polyacrylamide gel) and ArfA-GFP mutants revealed with an anti-GFP specific antibody. Identical amount of proteins were loaded in each lane as verified by immunoblotting with an anti-p64 rabbit antibody. (**B**) Histogram showing the percentage of wild-type (WT) cells, or cells expressing ArfA-Q71L-GFP and ArfA-T31N-GFP, with more than one nucleus. At least 50 cells were stained with DAPI and analyzed. (**C**) Histogram showing the percentage of WT cells, or cells expressing ArfA-Q71L-GFP and ArfA-T31N-GFP, with filopodia longer than 2 µm. At least 50 cells were fixed, stained with TRITC-phalloidin to visualize F-actin and analyzed using ImageJ to determine filopodia length. Experiments were repeated at least three times. *$P<0.05$. (**D**,**E**) Expression of ArfA-Q71L–GFP and ArfA-T31N–GFP was induced for 48 hours and cells labeled with anti-tubulin antibody. Perinuclear (indicated by arrows) and cytosolic localization was observed for ArfA mutants in interphase cells (upper rows). Neither ArfA-Q71L–GFP (D) or ArfA-T31N–GFP (E) proteins were enriched at the cleavage furrow (indicated by arrowheads). Scale bars: 5 µm.

mutant of Arf6 (Arf6-Q67L, GTP-bound) (Schweitzer and D'Souza-Schorey, 2002).

As previously described in cells constitutively expressing GFP-tagged ArfA (Guetta et al., 2010), ArfA-Q71L–GFP and ArfA-T31N–GFP mutants in interphase cells were mainly found in the perinuclear region and showed a diffuse cytosolic localization (Fig. 3D,E). In mitotic cells, neither ArfA-Q71L–GFP nor ArfA-T31N–GFP was enriched at the cleavage furrow; instead partial colocalization with tubulin was observed at the spindle poles for both forms. Although a transient concentration of ArfA at the cleavage furrow may have been overlooked, these localization studies do not support a direct function of ArfA during the abscission step. As described for Arf6 (D'Souza-Schorey and Chavrier, 2006), ArfA might nevertheless play a role in cytokinesis by regulating for instance membrane trafficking processes.

acapA$^-$ cells show reduced motility and streaming

When monitoring mitosis, we noticed that *acapA*$^-$ cells were less motile than wild-type cells. To further examine motility, cells moving randomly on glass coverslips were imaged every 30 seconds for 30 minutes and 50 cells were analyzed. Mutant *acapA*$^-$ cells moved 5.4±2.9 µm from their initial positions whereas WT and *acapA*$^-$ + ACAP-A–GFP cells moved 36.7±10.6 and 38.1±12.9 µm, respectively (Fig. 4A). This was accounted for by a marked difference in instantaneous speed: *acapA*$^-$ cells moved at 1.9±0.7 µm/minute while wild-type cells moved at 5.1±0.6 µm/minute and complemented *acapA*$^-$ cells at 4.7±0.6 µm/minute (data not shown). No migration defects were observed in *acapB*$^-$ cells (supplementary material Fig. S1B).

The motility defect of vegetative *acapA*$^-$ cells prompted us to examine whether multicellular development of starved cells was altered in these cells. We first followed motility of individual cells incubated in phosphate starvation buffer. Whereas motility was still defective in *acapA*$^-$ cell after one hour of starvation (data not shown), WT and *acapA*$^-$ cells moved respectively 61.9±21.2 µm and 56.5±17.2 µm from their initial positions after 10 hours (Fig. 4B), thus indicating that motility was restored in *acapA*$^-$ cells during development.

We next observed by microscopy collective movement of cells incubated into phosphate buffer in submerged conditions (supplementary material Fig. S3A). After 10 hours, WT cells

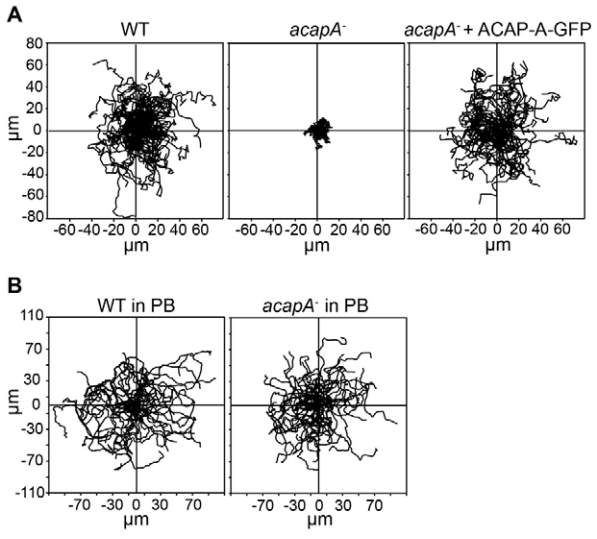

Fig. 4. Cell motility defect of *acapA*$^-$ cells. (**A**,**B**) The indicated cells were incubated in HL5 medium (A) or in phosphate buffer (PB) (B) for 10 hours and imaged on an Axiovert 200 inverted microscope. Randomly moving cells were imaged every 30 seconds for 30 minutes. Tracks of 50 randomly sampled cells are shown centred at the origin. Motility was restored in *acapA*$^-$ cells during early development.

gathered into streams moving towards aggregation centers. Aggregates were then clearly individualized after 14 hours. Streaming and aggregation was also observed with *acapA*$^{-}$ cells but with a delay of 4 hours in comparison to wild-type cells. To observe the late stage of development, cells were then plated on solid starvation plates. Development of WT cells was complete after 24 hours whereas *acapA*$^{-}$ cells showed fruiting body structures with morphology comparable to wild-type cells only after 36 hours (supplementary material Fig. S3C). In addition, spore yield and viability were not affected in *acapA*$^{-}$ cells (data not shown). This last result suggests that double deletion of both acapA and acapB genes might be required to observe spore production defects previously reported in *acapA*$^{-}$/*B*$^{-}$ cells (Chen et al., 2010).

Together our data suggest that ACAP-A does not affect chemotaxis or development. During development, mutant cells appear to migrate through a mechanism independent of ACAP-A. The time delay of the development cycle observed in the absence of ACAP-A might be due to defective migration until this ACAP-A-independent migration mechanism proceeds and/or ACAP-A control is released. These results are in agreement with the previous report that *acapA*$^{-}$, *acapB*$^{-}$ and *acapA*$^{-}$/*B*$^{-}$ cells show a normal multicellular development (Chen et al., 2010).

Altered cell shape and organization of F-actin in *acapA*$^{-}$ cells

The poor motility of *acapA*$^{-}$ cells strongly suggested that the remodeling of the actin cytoskeleton might be defective in these cells since actin-driven membrane protrusions are important for cell migration. To determine the effect of ACAP-A on cell shape and organization of F-actin, cells were labeled with TRITC-phalloidin to visualize F-actin (Fig. 5A). We also examined cell morphology by scanning electron microscopy (Fig. 5B). In contrast to WT and *acapB*$^{-}$ cells (supplementary material Fig.

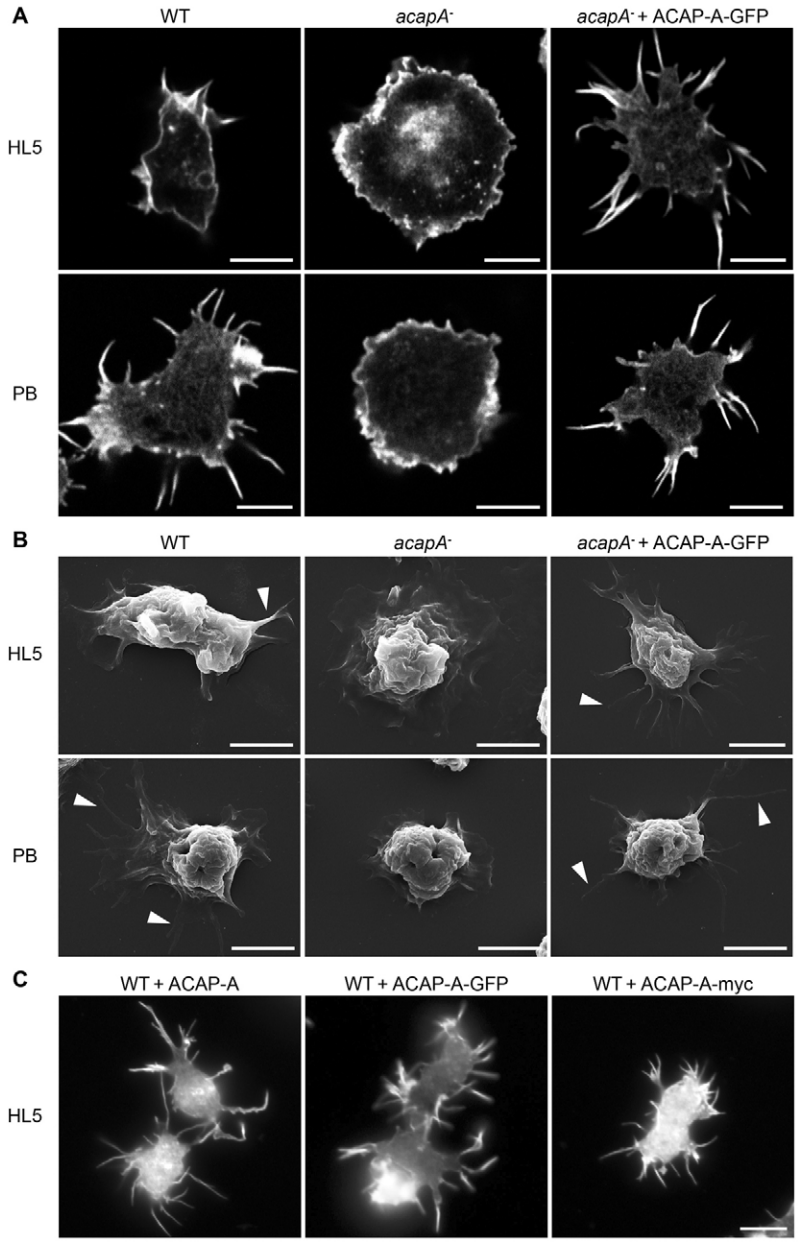

Fig. 5. Shape and organization of F-actin in *acapA*$^{-}$ cells. (**A–C**) The indicated cells were labeled with TRITC-phalloidin to visualize F-actin and observed by confocal microscopy (A) or by epifluorescence microscopy (C). Cells were also examined by scanning electron microscopy (B). *acapA*$^{-}$ cells showed severe defects in filopodia formation whereas cells expressing ACAP-A–GFP had more and considerably longer filopodia (indicated by arrowheads) than normally observed in wild-type cells. Expression of ACAP-A–GFP, myc-tagged ACAP-A (ACAP-A–myc) or untagged ACAP-A in wild-type cells also induced numerous long filopodia, suggesting that overexpression of ACAP-A has a dominant effect on filopodia morphogenesis independently of the epitope tag (GFP or myc). Scale bars: 5 μm.

S1C,D), *acapA*$^{-}$ cells showed severe defects in filopodia morphology and number. Instead of filopodia, they mainly displayed numerous membrane folds and lamellipodia (Fig. 5A,B). In culture medium (HL5), 100% of *acapA*$^{-}$ cells had no filopodia at all or less than six filopodia in contrast to WT cells which showed 75% of cells with less than six filopodia per cell (Fig. 6B). Furthermore, in WT cells 14% of filopodia were longer than 2 μm whereas filopodia this size were not seen in *acapA*$^{-}$ cells (Fig. 6C). Conversely, transfection of GFP-tagged ACAP-A in *acapA*$^{-}$ cells complemented this defect and generated more numerous as well as considerably longer filopodia than usually observed in WT cells (Fig. 5A). Thus, 90% of *acapA*$^{-}$ + ACAP-A–GFP cells showed more than five filopodia whereas no *acapA*$^{-}$ cells and only 25% of WT cells did (Fig. 6B). In *acapA*$^{-}$ + ACAP-A–GFP cells, 71% of filopodia were longer than 2 μm in contrast to 14% in WT cells (Fig. 6C). Interestingly, expression of ACAP-A–GFP in WT cells also induced numerous long filopodia (Fig. 5C), suggesting that overexpression of ACAP-A–GFP has a dominant effect on filopodia morphogenesis. Note that expression of untagged or myc-tagged ACAP-A led to comparable results (Fig. 5C), suggesting that the effect observed was caused by overexpression of ACAP-A. Finally, expression of ACAP-B–GFP in *acapA*$^{-}$ cells did not restore filopodia biogenesis, further underlining the distinct functions of ACAP-A and ACAP-B (supplementary material Fig. S1E).

Incubation of *Dictyostelium* cells in phosphate buffer induces numerous thin filopodial extensions, which are not observed in some mutants defective in genes controlling actin cytoskeleton remodeling (Gebbie et al., 2004). In this condition, *acapA*$^{-}$ cells formed filopodia that were short (87% filopodia ≤2 μm) in comparison to those observed in WT cells (83% filopodia >2 μm) (Fig. 5A,B and Fig. 6B,C). Note that the number and length of filopodia induced by the expression of ACAP-A–GFP were also influenced by phosphate buffer incubation (Fig. 6B,C). Together these results indicate a specific requirement for ACAP-A but not ACAP-B in the biogenesis of filopodia.

Next, to determine the dynamics of filopodia formed upon expression of ACAP-A–GFP in *acapA*$^{-}$ cells, we monitored filopodia formation and retraction in live cells by time-lapse video microscopy (Fig. 7). Filopodia extended with instantaneous speed of 0.49±0.06 μm/second (n=10) in WT cells (Fig. 7A) and 0.55±0.11 μm/second (n=10) in *acapA*$^{-}$ + ACAP-A–GFP cells (Fig. 7B,C). As previously reported (Medalia et al., 2007), retraction was often associated with an early filopodia bending step (Fig. 7D). These long filopodia did not inhibit migration (Fig. 4A) and apparently extended soon after pseudopodia protrusion (data not shown). We conclude that ACAP-A–GFP overexpression do not interfere with normal filopodia dynamics and cell migration.

ACAP-A-regulated actin remodeling depends on its GAP activity

To test whether actin remodeling was dependent on the GAP activity of ACAP-A, we mutated a conserved arginine (mutation R633Q) known to be critical for ArfGAP activity (Mandiyan

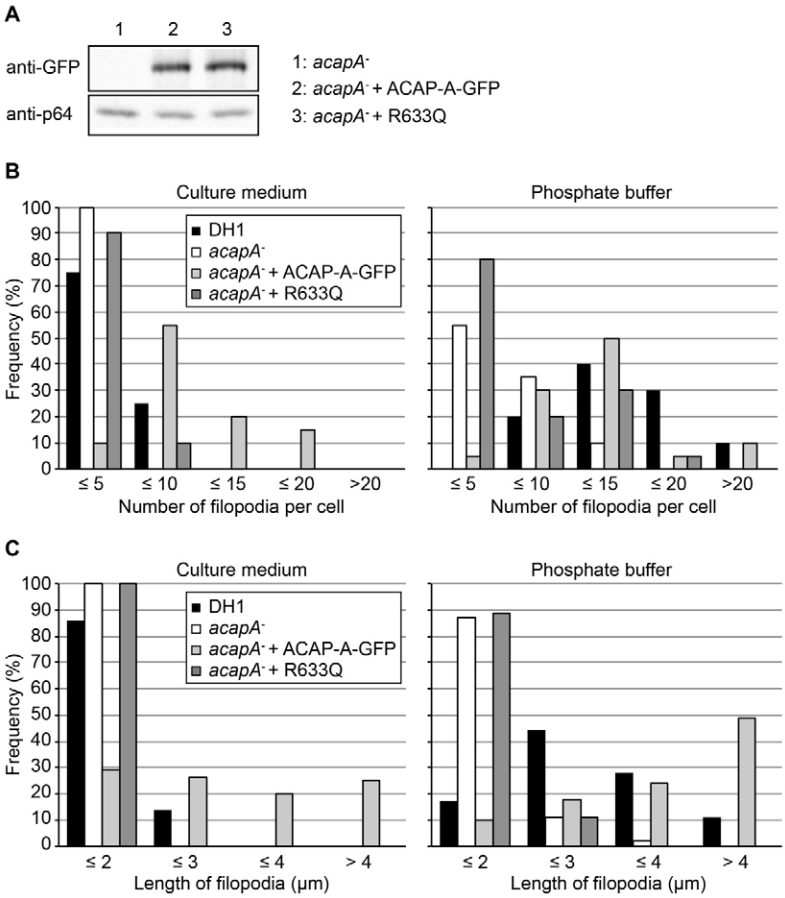

Fig. 6. Quantification of filopodia length and number in cells after ACAP-A deletion or ACAP-A–GFP overexpression. (**A**) ACAP-A-GFP and R633Q-ACAP-A–GFP were equally expressed in *acapA*$^{-}$ cells. Whole cell lysates (5×10^{5} cells/lane) were analyzed by electrophoresis (7% polyacrylamide gel) and ACAP-A–GFP proteins revealed with an anti-GFP specific antibody. Identical amounts of proteins were loaded in each lane as verified by immunoblotting with an anti-p64 rabbit antibody. (**B**) The number and (**C**) the length of actin protrusions longer than 1 μm in the indicated cells incubated in culture medium or for 1 hour in phosphate buffer were determined using ImageJ after cells were stained with TRITC-phalloidin to visualize F-actin (n=20 cells). Results are from one representative experiment repeated at least twice.

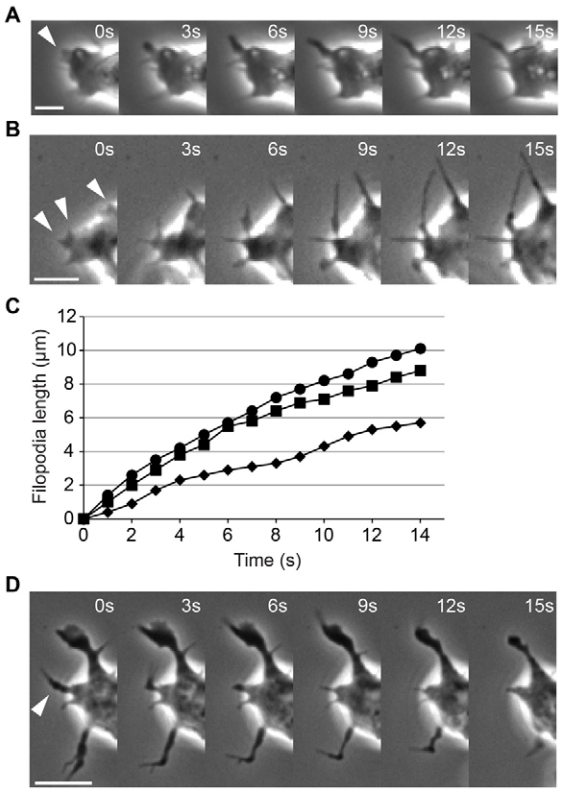

Fig. 7. Filopodia dynamics in live *acapA*$^{-}$ cells expressing ACAP-A–GFP. (**A**,**B**) Time-lapse series of phase contrast images of wild-type (A) and *acapA*$^{-}$ + ACAP-A–GFP (B) live cells showing filopodia extension (indicated by arrowheads). Live cells were imaged every second for 10 minutes on an Axiovert 200 inverted microscope. (**C**) Time course of the extension of the three filopodia indicated by arrowheads in B: the left (diamonds), the middle (square) and the right arrowheads (circle). Filopodia length was determined using the ImageJ. (**D**) Time-lapse series showing filopodia retraction (arrowhead) associated with early bending. ACAP-A–GFP overexpression in *acapA*$^{-}$ cells did not interfere with normal filopodia dynamics and cell migration. Scale bars: 5 μm.

et al., 1999; Randazzo et al., 2000; Szafer et al., 2000; Jackson et al., 2000). Protein expression level of mutant ACAP-A–GFP stably expressed in *acapA*$^{-}$ cells was comparable to that of ACAP-A–GFP (Fig. 6A). However this mutant did not restore filopodia formation (Fig. 6B,C) nor did it complement the cytokinesis defect (data not shown) in *acapA*$^{-}$ cells. This result strongly suggests a role of ArfA in filopodia biogenesis. This hypothesis was further comforted by the observation that expression of a constitutively activated ArfA•GTP mutant in WT cells led to a significant reduction of filopodia length in comparison to cells expressing a dominant negative ArfA•GDP mutant (Fig. 3C). Together these results suggest that the effect of ACAP-A on the actin cytoskeleton is GAP-activity dependent and likely associated to the control of ArfA•GTP level in cells.

ACAP-A is not enriched in filopodia

In vertebrates, ASAPs and ACAPs are associated with cytoskeleton structures (Inoue and Randazzo, 2007; Randazzo et al., 2007). To test whether ACAP-A function in filopodia biogenesis was linked to a hypothetic localization in membrane protrusions, first *acapA*$^{-}$ cells expressing ACAP–GFP were observed by confocal microscopy of live cells. When a confocal section was made within the cell body (CB, Fig. 8A,B), ACAP-A–GFP was seen in the cytosol and accumulated at the plasma membrane. In contrast, optical sections made at the level of the cell contact with the substratum (CS, Fig. 8A,C) revealed that ACAP-A–GFP was present but not concentrated in membrane protrusions. We next labeled fixed cells with TRITC-phalloidin to decorate F-actin. Colocalization of ACAP-A–GFP with cortical F-actin was observed (CB, Fig. 8D) whereas ACAP-A–GFP was not concentrated in filopodial F-actin-rich structures. This suggests that ACAP-A might not be directly required for the elongation of filopodial actin filaments or membrane deformation. Note that a transient accumulation (undetected in this study) of ACAP-A–GFP to filopodia cannot be formally excluded.

Loss of ACAP-A induces similar phenotypes in AX2 and DH1 strains

Our results indicating that ACAP-A plays a role in cytokinesis, cell motility and actin cytoskeleton remodeling were in apparent contradiction with a previous study that did not identify any such role for ACAP-A (Chen et al., 2010). Since these differences may be caused by the use of a different parental strain (AX2 versus DH1), we also deleted ACAP-A in AX2, the parental strain used in this previous work. Hereafter deleted strains are referred to as AX2-*acapA*$^{-}$ and DH1-*acapA*$^{-}$ cells, respectively.

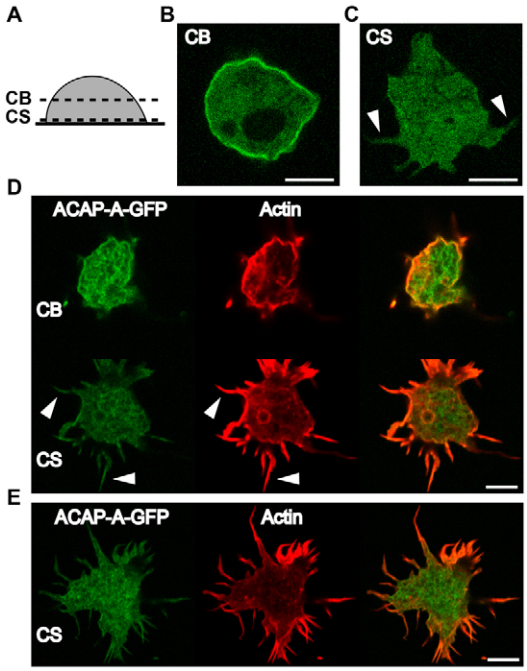

Fig. 8. Cellular localization of ACAP-A–GFP expressed in *acapA*$^{-}$ cells. (**A**) Confocal pictures were taken within the cell body (CB) or just at the level of the contact with the substrate (CS) as shown in the diagram. (**B**,**C**) Two different *acapA*$^{-}$ + ACAP-A–GFP cells were imaged by confocal microscopy of live cells. ACAP-A–GFP was seen in the cytosol and accumulated at the plasma membrane (B) but was not concentrated in membrane protrusions (C, indicated by arrowheads). (**D**,**E**) Two distinct cells were labeled with TRITC-phalloidin to visualize F-actin. ACAP-A–GFP did not accumulate in filopodia (indicated by arrowheads) but colocalized with cortical F-actin. Scale bars: 5 μm.

As expected, ACAP-A was not detected by western blotting in AX2-*acapA*$^{-}$ cells (supplementary material Fig. S1F). DAPI staining of fixed cells revealed that 45.8% of AX2-*acapA*$^{-}$ cells grown on plastic dishes exhibited two or more nuclei, a feature observed only in 2.4% of AX2 cells (supplementary material Fig. S1G). Only 12.1% of AX2-*acapA*$^{-}$ cells contained more than three nuclei against 52.8% of DH1-*acapA*$^{-}$ cells (Fig. 1D). Thus ACAP-A gene disruption in AX2 leads to a cytokinesis defect less pronounced than in DH1 cells, a phenotype that may be missed if not specifically tested. AX2-*acapA*$^{-}$ cells grown in suspension also exhibited a cytokinesis defect (supplementary material Fig. S1G). Next, we observed that AX2-*acapA*$^{-}$ cells were hardly motile, with an instantaneous speed of 1.1 ± 0.3 μm/minute while parental AX2 cells that moved at 3.9 ± 0.6 μm/minute (supplementary material Fig. S1H). Motility of AX2-*acapA*$^{-}$ cells was restored during development since streaming and aggregation were observed with only minor time delays compared to AX2 cells (supplementary material Fig. S3B,D). After 24 hours of development, both AX2 and AX2-*acapA*$^{-}$ cells showed fruiting bodies with comparable morphologies (supplementary material Fig. S3D). Finally, the organization of F-actin was analyzed in cells labeled with TRITC-phalloidin (supplementary material Fig. S1I–L). In culture medium (HL5), 100% of AX2-*acapA*$^{-}$ cells showed less than six filopodia against 45% of AX2 cells (supplementary material Fig. S1J). Whereas 47% of filopodia were longer than 2 μm in AX2 cells, such long filopods were not observed in AX2-*acapA*$^{-}$ cells (supplementary material Fig. S1K). This defect in AX2-*acapA*$^{-}$ cells was further amplified upon cell incubation in phosphate buffer for one hour. AX2-*acapA*$^{-}$ cells still formed short filopodia (90% filopodia $\leq$2 μm) while AX2 cells mainly showed long filopodia (86% filopodia $>$2 μm) (supplementary material Fig. S1K). Remarkably, after 6 hours of incubation in nutrient-depleted phosphate buffer, AX2-*acapA*$^{-}$ cells showed numerous cortical spike-like protrusions ($<$1 μm) whereas AX2 cells still displayed long filopodia (supplementary material Fig. S1L). This result is in agreement with actin remodeling defects previously noticed in *acapA*$^{-}$/*B*$^{-}$ cells after 5–6 hours of starvation (Chen et al., 2010).

We conclude that defects observed in *acapA*$^{-}$ cells were identically observed in two parental *Dictyostelium* strains, further reinforcing the role of ACAP-A in cytokinesis and actin cytoskeleton dynamics. Partial discrepancies between our results and those of Chen and co-workers are discussed below.

Discussion

In this study, we report the function of an Arf-GTPase activating protein, ACAP-A, in the model organism *Dictyostelium discoideum*. We demonstrate for the first time that inactivation of the gene coding for ACAP-A results in strong phenotypes, including cytokinesis defects, reduced motility and impaired actin cytoskeleton remodeling. We provide the first evidence that the GAP domain is essential for these functions suggesting that ACAP-A regulates the actin skeleton organization and dynamics in an ArfA-dependent manner.

ACAP-A and cytokinesis

In mammalian cells, Arf6 is required for cytokinesis (D'Souza-Schorey and Chavrier, 2006). Hence overexpression of Arf6•GTP (Brown et al., 2001) and depletion of Arf6 using siRNA (Schweitzer and D'Souza-Schorey, 2002) cause cytokinesis defects. In addition, depletion of ACAP1, a GAP for Arf6 that is highly homologous to ACAP-A (Chen et al., 2010), impairs cytokinesis and leads to the accumulation of binucleated cells (Rueckert and Haucke, 2012). Here in *Dictyostelium*, cytokinesis defects were comparably observed when manipulating ArfA activity. This was first achieved by interfering with the GAP activity of ACAP-A. Indeed, in cells deprived of ACAP-A (*acapA*$^{-}$ cells) inferred excess of ArfA•GTP was associated with concomitant cytokinesis defects. ArfA activity was also altered in cells by overexpression of a constitutively active mutant of ArfA (ArfA•GTP) and this led to cells with multiple nuclei.

What is the function of ArfA and ACAP-A in cytokinesis? Our microscopy studies did not allow to identify a particular localization for ArfA and ACAP-A that would indicate an obvious function in cytokinesis, for instance in cleavage furrow ingression. In mammalian cells, Arf6•GTP localizes to the cleavage furrow and the midbody in mitotic cells (Schweitzer and D'Souza-Schorey, 2002). Numerous studies on Arf6 strongly indicate that this GTPase regulates endosomal trafficking events crucial for cytokinesis (Schweitzer et al., 2011; McKay and Burgess, 2011; D'Souza-Schorey and Chavrier, 2006). In *Dictyostelium*, ArfA is the only ArfGTPase (Weeks et al., 2005; Chen et al., 2010) and thus, functions in the endocytic or secretory pathways controlled by individual members of the three different mammalian Arf classes might be supported by ArfA alone in amoeba. To our knowledge, the role of ArfA in endosomal trafficking has never been assessed, although ArfA•GDP was reported to associate with an arrestin related protein localized to endocytic compartments (Guetta et al., 2010) and ArfA was also identified as a phagosomal protein (Gotthardt et al., 2006). ArfA is highly homologous to human Arf1 (Weeks et. al., 2005; Chen et al., 2010) known to regulate membrane trafficking in the secretory pathway. In mammalian cells, secretory Golgi-derived vesicles traffic to the cleavage furrow and the midbody region during cytokinesis (Goss and Toomre, 2008). Consistent with the localization of ArfA to the Golgi apparatus (Guetta et al., 2010), the role of ArfA in cytokinesis might be related to hypothetical functions in the secretory pathway and Golgi structure. This hypothesis does not exclude that ArfA (and ACAP-A) might also be required for the control of actin remodeling during cytokinesis.

ACAP-A and cell migration

For the first time we report here that ACAP-A participates in vegetative *Dictyostelium* cell migration. In mammalian cells, downregulation as well as overexpression of the Arf6 GAP ACAP1 has been shown to inhibit migration induced by stimulation-dependent recycling of integrin β and controls of Arf6•GTP levels (Li et al., 2005; Ma et al., 2007). The role of Arf6 in cell migration is known to rely on its capacity to regulate internalization and trafficking of integrins but also to remodel the actin cytoskeleton notably via Rac1 trafficking to the plasma membrane (Schweitzer et al., 2011; D'Souza-Schorey and Chavrier, 2006). In *Dictyostelium*, Rac1 GTPases appear to regulate cell motility (Dumontier et al., 2000; Filić et al., 2011) and therefore ACAP-A might participate in Rac1 localization that will regulate subsequently actin cytoskeleton dynamics. Interestingly, during *Dictyostelium* development, ACAP-A does not regulate cell motility since motility was restored in *acapA*$^{-}$ cells upon starvation. This suggests that the migration machinery

might be controlled by ArfA/ACAP-A independent signals during development.

ACAP-A and actin cytoskeleton remodeling

Multi-domain ArfGAPs have been shown to regulate membrane remodeling associated to actin polymerization (Randazzo and Hirsch, 2004; Randazzo et al., 2007). Here we provide evidence that ACAP-A regulates actin cytoskeleton remodeling in *Dictyostelium*. First, deletion of ACAP-A impairs membrane protrusions usually observed in vegetative *Dictyostelium* cells. Second, overexpression of ACAP-A in *acapA*$^-$ cells induces the formation of numerous long filopodia. In addition, we show here that actin remodeling is dependent on the GAP activity of ACAP-A since a GAP defective ACAP-A mutant (ACAP-A R633Q) expressed in *acapA*$^-$ cells does not restore filopodia formation. Therefore the effect of ACAP-A on actin remodeling appears as an Arf-dependent activity and consequently might be associated to well-known Arf functions such as the regulation of Rho family GTPases that control actin dynamics (Schweitzer et al., 2011; McKay and Burgess, 2011; D'Souza-Schorey and Chavrier, 2006). Hence, ArfA might control actin polymerization by positive regulation of Rac1, which in turn would activate dDia2 responsible for filopodia elongation (Schirenbeck et al., 2005). In agreement with the hypothetical Arf-dependent function of ACAP-A, we observe that overexpression of a constitutively activated ArfA•GTP mutant leads to a significant reduction of filopodia length. However the extent of this reduction is modest in comparison to that observed in *acapA*$^-$ cells in which ArfA•GTP is inferred to accumulate. Furthermore, overexpression of a dominant negative ArfA•GDP mutant, a situation that should mimic ACAP-A overexpression, does not enhance filopodia protrusions. Together these observations suggest that ACAP-A could have additional Arf-independent activities that affect actin cytoskeleton. ACAP-A might play for instance a direct role in actin nucleation during filopodia formation. However in contrast to dDia2, a known actin nucleator localized at the tips of filopodia (Schirenbeck et al., 2005), ACAP-A–GFP is apparently not enriched in these domains, unless this localization is too transient to be detected or is masked by the overexpression of the GFP-tagged protein. Alternatively, ACAP-A might participate in membrane deformation associated to filopodia extension. Such a role has been described for proteins with an IMD domain (IRSp53 and MIM homology Domain) similar to the BAR/I-BAR domain that functions both as a sensor and inducer of membrane curvature (Ahmed et al., 2010; Rao and Haucke, 2011). Indeed, overexpression of the IMD domain of IRSp53 can induce filopodia-like structures and other domains of IRSp53 interact with several key players in actin dynamics (e.g. WAVE, N-WASP, mDia1) suggesting that IRSp53 participates in the mechanism of filopodia formation (Ahmed et al., 2010). Interestingly, ACAP-A contains a BAR domain that might share similar functions with the IMD domain of IRSp53. However, the apparent cortical localization of ACAP-A–GFP does not support this hypothesis. Alternatively, the BAR domain (maybe interacting with the PH domain) could regulate the association of ACAP-A with membranes enriched in ArfA or might affect the GAP enzymatic activity as reported for the ArfGAP ASAP1 (Jian et al., 2009). Additional experiments will be further required to test these hypothesis and determine critical domains of ACAP-A required for theses GAP-independent functions.

Comparison to previous studies on *Dictyostelium* ACAP-A

Finally, as mentioned above, there are apparent discrepancies between our study and previously published results (Chen et al., 2010), since we demonstrate that the deletion of ACAP-A is sufficient to induce dramatic defects in vegetative cells that were unnoticed in this early work. However, upon close examination, the vast majority of the differences between our results and this previous study appear to reflect differences in the phenotypes analyzed in both studies. First, the cytokinesis defect in *acapA*$^-$ cells was not described in this previous study. Here we report that AX2-*acapA*$^-$ cells exhibit a cytokinesis defect, but less pronounced than in DH1-*acapA*$^-$ cells. Thus the cytokinesis defect in AX2-*acapA*$^-$ cells might be only revealed upon careful quantitative analysis of DAPI stained nuclei, which is not a routine procedure in all laboratories. Second, we noticed a strong motility defect in *acapA*$^-$ cells that had not been reported before. In our hands, this defect was observed both in AX2-*acapA*$^-$ and DH1-*acapA*$^-$ cells but time-lapse microscopy studies were required to uncover these cell migration defects. However, we observed a nearly normal motility of *acapA*$^-$ cells during development, which is in agreement with previous results reporting normal chemotaxis, streaming and development in *acapA*$^-$/*B*$^-$ cells (Chen et al., 2010). Third, the reduced number and length of filopodia in vegetative *acapA*$^-$ cells was not previously observed, whereas we demonstrate here that both AX2-*acapA*$^-$ and DH1-*acapA*$^-$ cells have a similar defect in actin remodeling. However this anomaly is most striking when cells are incubated in phosphate buffer for one hour, a condition that was not analyzed previously. Conversely, Chen and co-workers analyzed actin cytoskeleton of cells during development (5–6 hours of starvation) and reported that *acapA*$^-$/*B*$^-$ cells display a greater number of short actin protrusions in comparison to wild-type cells (Chen et al., 2010), a phenotype also observed in this study. In summary, no significant contradiction is noticeable between our results and previously published results. It is likely that defects associated with inactivation of ACAP-A were overlooked because they were not apparent in the assays used previously (Chen et al., 2010).

Materials and Methods

Cell culture, antibodies, gel electrophoresis and immunoblotting

D. discoideum strains DH1-10 (Cornillon et al., 2000) and AX2 were grown at 22°C in HL5 medium and subcultured twice a week. Mouse monoclonal antibody (mAb) against p25 (H72) was described previously (Mercanti et al., 2006). mAb to GFP and myc (9E10) were purchased (Roche Diagnostics, Meylan, France). mAb to alpha tubulin (DM1A), 4′,6-diamidino-2-phenylindole (DAPI) and tetramethylrhodamine B isothiocyanate (TRITC)-labeled phalloidin were from Sigma-Aldrich (St Quentin Fallavier, France). Polyclonal antibodies to ACAP-A and p64 (DDB_G0282233) were raised in rabbits using KLH-coupled peptides (^{1063}EKDKDYKNTRPKSK^{1076}; ^{1311}NKKPKKSKKSKPLE^{1324}) and GST-p64 (residues 427–522) recombinant protein, respectively (Covalab, Villeurbanne, France). The anti-ACAP-A antibody did not generate a signal in immunofluorescence experiments (data not shown). SDS polyacrylamide electrophoresis and immunoblotting were performed as previously described (Cornillon et al., 2000). Bands were detected by ECL (Thermo Scientific, Courtaboeuf, France) and a ChemiDoc MP imager (Bio-Rad, Marnes-la-Coquette, France).

Immunofluorescence microscopy

For immunofluorescence analysis, cells were applied on glass coverslips overnight, incubated or not in phosphate buffer (PB, 2 mM Na_2HPO_4, 14.7 mM KH_2PO_4, pH 6.5) then fixed with 4% paraformaldehyde for 30 minutes, washed and permeabilized with methanol at −20°C for 2 minutes. Cells were incubated with

the indicated antibodies for 1 hour, and then stained with corresponding fluorescent (Alexa Fluor 488/568) secondary antibodies (Molecular Probes/Invitrogen, Eugene, OR) for 30 minutes. The actin cytoskeleton was labeled by incubating paraformaldehyde-fixed cells for 1 hour in phosphate-buffered saline (PBS) containing 0.2% BSA and 1 µg/ml (TRITC)-labeled phalloidin. Cells were observed by laser scanning confocal microscopy (Zeiss LSM 510 Meta) or epifluorescence microscopy (Zeiss AxioImager Z1) when indicated. For nuclei staining, cells were treated as described above, incubated with DAPI for 30 minutes and observed with a Zeiss AxioImager Z1 photomicroscope.

Scanning electron microscopy

For scanning electron microscopy, cells were incubated on glass coverslides overnight in HL5. Cells were then incubated or not in PB for 1 hour before fixation using 2% glutaraldehyde in HL5 for 30 minutes followed by 2% glutaraldehyde in 100 mM PB (pH 7.14) for 30 minutes. Cells were rinsed and postfixed in 1% osmium tetroxide in 100 mM PB (pH 7.14) for 1 hour. The fixative was removed, and cells were progressively dehydrated through a 25–100% ethanol series. After air-drying, cells were sputter-coated in gold and viewed on a JEOL-JSM-7001 FA Field Emission Scanning Electron Microscope.

Live cell imaging and analysis

Cells were incubated overnight in Lab-Tek (Nalgene) chambered coverglasses in HL5 medium and imaged on an Axiovert 200 inverted microscope with a motorized stage. Randomly moving cells were imaged every 30 seconds for 30 minutes. Films were processed by manual centroid tracking of at least 50 cells with the ImageJ analysis software (NIH) and MTrackJ. For mitosis analysis, asynchronously grown cells were imaged every 15 seconds for 1 hour. To document filopodia dynamics, cells were identically imaged every second for 10 minutes.

Plasmids and cell transfection

Full-length ACAP-A and mutants were produced by PCR using pairs of oligonucleotides containing *Bam*HI and *Xho*I sites in 5′ and 3′, respectively. PCR fragments were digested by *Bam*HI and *Xho*I and cloned into *Bam*HI/*Xho*I sites of pDXA-3C (Manstein et al., 1995) containing either GFP or a triple myc-tag for C-terminal fusion. All constructs were sequenced (Genome express, Grenoble, France). Plasmids were linearized by **Sca**I and transfected in *Dictyostelium* by electroporation as described (Cornillon et al., 2000). Clone selection was made with 10 mg/ml G418. ArfA(Q71L) and ArfA(T31N) mutants (kindly provided by Dr Laurence Aubry, CEA, Grenoble, France) were subcloned after PCR amplification into *Bgl*II/*Spe*I sites of the inducible expression vector pDM370 (Veltman et al., 2009). After electroporation, transfectants were selected and maintained in 25 µg/ml hygromycin. Expression was induced by adding 10 µg/ml doxycycline 2 or 3 days before analysis.

acapA knockout cells

To obtain the *acapA* knockout vector, the 5′ fragment was amplified from genomic DNA with sens (ATGAGTGGGCAACAACCAACAACAGAA) and antisens (CATTTGATCATTAATACTATTAACAGA) oligonucleotides and cloned into pBlueScript vector (Stratagene, La Jolla, CA). The 3′ fragment was obtained by PCR using sense (GAATTTCATCCAGAAAATGCATTAAAT) and antisense (TGGATCAACCAATGTAATGTCAGCACC) oligonucleotides and cloned in pBlueScript containing the 5′ fragment. After sequencing, the knockout vector was completed by inserting the blasticidin resistance cassette between the two 5′ and 3′ fragments. The resulting plasmid was linearized by digestion with restriction enzymes (*Kpn*I and *Not*I) and electroporated into DH1-10 cells. Transformants were selected in presence of 10 µg/ml blasticidin. Individual colonies were tested by PCR and the absence of expression ACAP-A mRNA was then verified by RT-PCR. The ACAP-A mutant retains residues 1–273 from the complete amino sequence, leaving thus only half of the BAR domain (102 out of 229 residues).

Acknowledgements

We thank Laurence Aubry (U1038 Inserm/CEA/UJF CEA, Grenoble, France) for her generous gift of ArfA constructs and Christophe Anjard (UMR5534, Lyon, France) for helpful suggestions.

Funding

This work was supported by grants from the Association pour la Recherche contre le Cancer (ARC) [grant number 1082 to F.L.]; and the research program of the Région Rhône-Alpes (to F.L.). P.C.'s laboratory is funded by the Fonds National Suisse pour la Recherche Scientifique.

Supplementary material available online at
http://jcs.biologists.org/lookup/suppl/doi:10.1242/jcs.113951/-/DC1

References

Ahmed, S., Goh, W. I. and Bu, W. (2010). I-BAR domains, IRSp53 and filopodium formation. *Semin. Cell Dev. Biol.* **21**, 350-356.

Block, J., Breitsprecher, D., Kühn, S., Winterhoff, M., Kage, F., Geffers, R., Duwe, P., Rohn, J. L., Baum, B., Brakebusch, C. et al. (2012). FMNL2 drives actin-based protrusion and migration downstream of Cdc42. *Curr. Biol.* **22**, 1005-1012.

Breitsprecher, D., Jaiswal, R., Bombardier, J. P., Gould, C. J., Gelles, J. and Goode, B. L. (2012). Rocket launcher mechanism of collaborative actin assembly defined by single-molecule imaging. *Science* **336**, 1164-1168.

Brown, F. D., Rozelle, A. L., Yin, H. L., Balla, T. and Donaldson, J. G. (2001). Phosphatidylinositol 4,5-bisphosphate and Arf6-regulated membrane traffic. *J. Cell Biol.* **154**, 1007-1018.

Chen, P. W., Randazzo, P. A. and Parent, C. A. (2010). ACAP-A/B are ArfGAP homologs in dictyostelium involved in sporulation but not in chemotaxis. *PLoS ONE* **5**, e8624.

Cornillon, S., Pech, E., Benghezal, M., Ravanel, K., Gaynor, E., Letourneur, F., Brückert, F. and Cosson, P. (2000). Phg1p is a nine-transmembrane protein superfamily member involved in dictyostelium adhesion and phagocytosis. *J. Biol. Chem.* **275**, 34287-34292.

D'Souza-Schorey, C. and Chavrier, P. (2006). ARF proteins: roles in membrane traffic and beyond. *Nat. Rev. Mol. Cell Biol.* **7**, 347-358.

Donaldson, J. G. and Jackson, C. L. (2011). ARF family G proteins and their regulators: roles in membrane transport, development and disease. *Nat. Rev. Mol. Cell Biol.* **12**, 362-375.

Dumontier, M., Höcht, P., Mintert, U. and Faix, J. (2000). Rac1 GTPases control filopodia formation, cell motility, endocytosis, cytokinesis and development in Dictyostelium. *J. Cell Sci.* **113**, 2253-2265.

Faix, J. and Rottner, K. (2006). The making of filopodia. *Curr. Opin. Cell Biol.* **18**, 18-25.

Faix, J., Breitsprecher, D., Stradal, T. E. and Rottner, K. (2009). Filopodia: Complex models for simple rods. *Int. J. Biochem. Cell Biol.* **41**, 1656-1664.

Filić, V., Marinović, M., Faix, J. and Weber, I. (2012). A dual role for Rac1 GTPases in the regulation of cell motility. *J. Cell Sci.* **125**, 387-398.

Gebbie, L., Benghezal, M., Cornillon, S., Froquet, R., Cherix, N., Malbouyres, M., Lefkir, Y., Grangeasse, C., Fache, S., Dalous, J. et al. (2004). Phg2, a kinase involved in adhesion and focal site modeling in Dictyostelium. *Mol. Biol. Cell* **15**, 3915-3925.

Gillingham, A. K. and Munro, S. (2007). The small G proteins of the Arf family and their regulators. *Annu. Rev. Cell Dev. Biol.* **23**, 579-611.

Goss, J. W. and Toomre, D. K. (2008). Both daughter cells traffic and exocytose membrane at the cleavage furrow during mammalian cytokinesis. *J. Cell Biol.* **181**, 1047-1054.

Gotthardt, D., Blancheteau, V., Bosserhoff, A., Ruppert, T., Delorenzi, M. and Soldati, T. (2006). Proteomics fingerprinting of phagosome maturation and evidence for the role of a Galpha during uptake. *Mol. Cell. Proteomics* **5**, 2228-2243.

Guetta, D., Langou, K., Grunwald, D., Klein, G. and Aubry, L. (2010). FYVE-dependent endosomal targeting of an arrestin-related protein in amoeba. *PLoS ONE* **5**, e15249.

Gupton, S. L. and Gertler, F. B. (2007). Filopodia: the fingers that do the walking. *Sci. STKE* **2007**, re5.

Inoue, H. and Randazzo, P. A. (2007). Arf GAPs and their interacting proteins. *Traffic* **8**, 1465-1475.

Jackson, T. R., Brown, F. D., Nie, Z., Miura, K., Foroni, L., Sun, J., Hsu, V. W., Donaldson, J. G. and Randazzo, P. A. (2000). ACAPs are arf6 GTPase-activating proteins that function in the cell periphery. *J. Cell Biol.* **151**, 627-638.

Jian, X., Brown, P., Schuck, P., Gruschus, J. M., Balbo, A., Hinshaw, J. E. and Randazzo, P. A. (2009). Autoinhibition of Arf GTPase-activating protein activity by the BAR domain in ASAP1. *J. Biol. Chem.* **284**, 1652-1663.

Kahn, R. A., Bruford, E., Inoue, H., Logsdon, J. M., Jr, Nie, Z., Premont, R. T., Randazzo, P. A., Satake, M., Theibert, A. B., Zapp, M. L. et al. (2008). Consensus nomenclature for the human ArfGAP domain-containing proteins. *J. Cell Biol.* **182**, 1039-1044.

Kanno, E., Ishibashi, K., Kobayashi, H., Matsui, T., Ohbayashi, N. and Fukuda, M. (2010). Comprehensive screening for novel rab-binding proteins by GST pull-down assay using 60 different mammalian Rabs. *Traffic* **11**, 491-507.

Kerber, M. L. and Cheney, R. E. (2011). Myosin-X: a MyTH-FERM myosin at the tips of filopodia. *J. Cell Sci.* **124**, 3733-3741.

Kobayashi, H. and Fukuda, M. (2012). Rab35 regulates Arf6 activity through centaurin-β2 (ACAP2) during neurite outgrowth. *J. Cell Sci.* **125**, 2235-2243.

Li, J., Ballif, B. A., Powelka, A. M., Dai, J., Gygi, S. P. and Hsu, V. W. (2005). Phosphorylation of ACAP1 by Akt regulates the stimulation-dependent recycling of integrin beta1 to control cell migration. *Dev. Cell* **9**, 663-673.

Li, J., Peters, P. J., Bai, M., Dai, J., Bos, E., Kirchhausen, T., Kandror, K. V. and Hsu, V. W. (2007). An ACAP1-containing clathrin coat complex for endocytic recycling. *J. Cell Biol.* **178**, 453-464.

Ma, Z., Nie, Z., Luo, R., Casanova, J. E. and Ravichandran, K. S. (2007). Regulation of Arf6 and ACAP1 signaling by the PTB-domain-containing adaptor protein GULP. *Curr. Biol.* **17**, 722-727.

Mandiyan, V., Andreev, J., Schlessinger, J. and Hubbard, S. R. (1999). Crystal structure of the ARF-GAP domain and ankyrin repeats of PYK2-associated protein beta. *EMBO J.* **18**, 6890-6898.

Manstein, D. J., Schuster, H. P., Morandini, P. and Hunt, D. M. (1995). Cloning vectors for the production of proteins in Dictyostelium discoideum. *Gene* **162**, 129-134.

Mattila, P. K. and Lappalainen, P. (2008). Filopodia: molecular architecture and cellular functions. *Nat. Rev. Mol. Cell Biol.* **9**, 446-454.

McKay, H. F. and Burgess, D. R. (2011). 'Life is a highway': membrane trafficking during cytokinesis. *Traffic* **12**, 247-251.

Medalia, O., Beck, M., Ecke, M., Weber, I., Neujahr, R., Baumeister, W. and Gerisch, G. (2007). Organization of actin networks in intact filopodia. *Curr. Biol.* **17**, 79-84.

Mellor, H. (2010). The role of formins in filopodia formation. *Biochim. Biophys. Acta* **1803**, 191-200.

Mercanti, V., Charette, S. J., Bennett, N., Ryckewaert, J. J., Letourneur, F. and Cosson, P. (2006). Selective membrane exclusion in phagocytic and macropinocytic cups. *J. Cell Sci.* **119**, 4079-4087.

Randazzo, P. A. and Hirsch, D. S. (2004). Arf GAPs: multifunctional proteins that regulate membrane traffic and actin remodelling. *Cell. Signal.* **16**, 401-413.

Randazzo, P. A., Andrade, J., Miura, K., Brown, M. T., Long, Y. Q., Stauffer, S., Roller, P. and Cooper, J. A. (2000). The Arf GTPase-activating protein ASAP1 regulates the actin cytoskeleton. *Proc. Natl. Acad. Sci. USA* **97**, 4011-4016.

Randazzo, P. A., Inoue, H. and Bharti, S. (2007). Arf GAPs as regulators of the actin cytoskeleton. *Biol. Cell* **99**, 583-600.

Rao, Y. and Haucke, V. (2011). Membrane shaping by the Bin/amphiphysin/Rvs (BAR) domain protein superfamily. *Cell. Mol. Life Sci.* **68**, 3983-3993.

Rueckert, C. and Haucke, V. (2012). The oncogenic TBC domain protein USP6/TRE17 regulates cell migration and cytokinesis. *Biol. Cell* **104**, 22-33.

Schirenbeck, A., Bretschneider, T., Arasada, R., Schleicher, M. and Faix, J. (2005). The Diaphanous-related formin dDia2 is required for the formation and maintenance of filopodia. *Nat. Cell Biol.* **7**, 619-625.

Schweitzer, J. K. and D'Souza-Schorey, C. (2002). Localization and activation of the ARF6 GTPase during cleavage furrow ingression and cytokinesis. *J. Biol. Chem.* **277**, 27210-27216.

Schweitzer, J. K., Sedgwick, A. E. and D'Souza-Schorey, C. (2011). ARF6-mediated endocytic recycling impacts cell movement, cell division and lipid homeostasis. *Semin. Cell Dev. Biol.* **22**, 39-47.

Steffen, A., Faix, J., Resch, G. P., Linkner, J., Wehland, J., Small, J. V., Rottner, K. and Stradal, T. E. (2006). Filopodia formation in the absence of functional WAVE- and Arp2/3-complexes. *Mol. Biol. Cell* **17**, 2581-2591.

Szafer, E., Pick, E., Rotman, M., Zuck, S., Huber, I. and Cassel, D. (2000). Role of coatomer and phospholipids in GTPase-activating protein-dependent hydrolysis of GTP by ADP-ribosylation factor-1. *J. Biol. Chem.* **275**, 23615-23619.

Veltman, D. M., Keizer-Gunnink, I. and Haastert, P. J. (2009). An extrachromosomal, inducible expression system for Dictyostelium discoideum. *Plasmid* **61**, 119-125.

Weeks, G., Gaudet, P. and Insall, R. H. (2005). The small GTPase superfamily. In *Dictyostelium Genomics* (ed. W. F. Loomis and A. Kuspa), pp. 173-201. Norfolk, UK: Horizon Bioscience.

Wood, W. and Martin, P. (2002). Structures in focus – filopodia. *Int. J. Biochem. Cell Biol.* **34**, 726-730.

Yang, C. and Svitkina, T. (2011). Filopodia initiation: focus on the Arp2/3 complex and formins. *Cell Adhes. Migr.* **5**, 402-408.